Title: Identification of novel flowering genes using RNA-Seq pipeline employing combinatorial approach in *Arabidopsis thaliana* time-series apical shoot meristem data

Abstract:

Floral transition is a crucial event in the reproductive cycle of a flowering plant during which many genes are expressed that govern the transition phase and regulate the expression and functions of several other genes involved in the process. Identification of additional genes connected to flowering genes is vital since they may regulate flowering genes and vice versa. Through our study, expression values of these additional genes has been found similar to flowering genes *FLC* and *LFY* in the transition phase. The presented approach plays a crucial role in this discovery. An RNA-Seq computational pipeline was developed for identification of novel genes involved in floral transition from *A. thaliana* apical shoot meristem time-series data. By intersecting differentially expressed genes from Cuffdiff, DESeq and edgeR methods, 690 genes were identified. Using FDR cutoff of 0.05, we identified 30 genes involved in glucosinolate and glycosinolate biosynthetic processes as principle regulators in the transition phase which provide protection to plants from herbivores and pathogens during flowering. Additionally, expression profiles of highly connected genes in protein-protein interaction network analysis revealed 76 genes with non-functional association and high correlation to flowering genes *FLC* and *LFY* which suggests their potential and principal role in floral regulation not identified previously in any studies.

Keywords: Apical shoot; Flowering; Pipeline; Cuffdiff; Step Analysis; Differential expression; Enrichment; *Arabidopsis Thaliana*

1. Background

RNA-Seq is now a frequently used method in plant biology. Studies using mutant analysis on *A.thaliana* have uncovered a range of genes involved in flowering (Koornneef, Hanhart and van der Veen, 1991). Analysis of *A. thaliana* apical shoot data suggest that certain known genes are commonly regulated during the transition phase (Klepikova *et al.*, 2015). Recent RNA-Seq studies on fruit plants such as blueberry have used Cuffdiff software (Trapnell *et al.*, 2012) with default parameters (Gupta *et al.*, 2015) to identify candidate genes. Similar studies have also been performed in *A. thaliana* using different computational approaches with default parameters for alternative splicing detection (Liu, Loraine and Dickerson, 2014). Many of these RNA-Seq studies focus on identification of differentially expressed genes (DEGs) using bioinformatics tools. However, very often these comparative studies fail to consider optimal parameters required for upstream processing of the data prior to DEG analysis. Due to this, RNA-Seq studies involving plants sometimes do not generate optimal results.

Accurate mapping of raw RNA-Seq reads is essential for identification of DEGs. A recent study by Zhao and Zhang (Zhao and Zhang, 2015) showed that divergent genesets can influence the outcome of the analysis. They characterized the impact of genome annotation choice on read mapping and transcript quantification by analyzing RNA-Seq datasets (Zhao and Zhang, 2015). In addition, certain parameters also affect mapping of reads to the transcriptome. For example, in the popular splice junction mapper TopHat2 (Kim *et al.*, 2013) there are parameters to control 'unique mapping' and 'mapping of concordant read pairs'. By changing the value of the 'unique mapping' parameter, reads are only aligned the specified number of times to the genome and therefore the overall mapping rate is affected. Similarly, by switching on the 'mapping of concordant read pairs' parameter, both read pairs map to the same sequence in correct orientation with suitable distance between them. Parameters such as 'maximum fragment length' also affect how the reads are mapped for paired-end reads. Default values of these parameters, which are designed for mammalian genomes, when applied in plants can result in the loss of paired reads that map further than certain default base pairs (bp). Therefore, using default parameters can lead to false positive results. Furthermore, commercial RNA-Seq software such as CLC Genomics fails to consider this aspect, which can lead to generation of unreliable results. Therefore, considering the impact of parameters on read mapping to identification of DEGs, a standardized computational pipeline is required.

In this study, we identified novel DEGs which can potentially regulate the function of flowering genes using a bioinformatics pipeline from plant RNA-Seq time-series data processing (Fig. 1). The pipeline which consisted of three components: data processing; Differential Gene Expression (DGE); and Gene Ontology (GO) annotation and enrichment, was applied to *A. thaliana* apical shoot data. We identified several thousand differentially expressed genes during the transition phase (i.e. from vegetative to reproductive developmental phase) by intersection of DGE results obtained from Cuffdiff, DESeq and edgeR tools. Expression profiles of the overlapped genes were studied and GO enrichment analysis was used to identify a list of novel candidate genes involved in flowering. Finally, we identified several genes with crucial protein interactions and potential roles in the regulation of flowering.

2. Methods

2.1 Data analysis pipeline

The pipeline workflow (Fig. 1), starts with conversion of reads in SRA format to FASTQ format as FASTQ files were needed for sequence alignment (Ostell and McEntyre, 2007). A quality metric report was generated using FastQC tool (Andrews, 2010) which briefly outlines metrics of sequence quality, quality scores, sequence content, sequence length distribution, sequence duplication levels, overrepresented sequences, adapter content and Kmer content. Based on the metrics, reads were trimmed to generate trimmed read files for each sample using Cutadapt (Martin, 2011). Following read trimming, samples were again checked for contaminated sequences, adapters, and poor-quality reads so that they could be removed before alignment. Sample reads were then each aligned to the *A. thaliana* genome using TopHat2 (Kim *et al.*, 2013) which is a fast splice junction mapper based on Bowtie2 (Langmead and Salzberg, 2012). Cufflinks and Cuffmerge were used for transcript assembly and transcript merging. DGE was performed using Cuffdiff (Trapnell *et al.*, 2012). For DGE analysis using DESeq and edgeR, BAM

files obtained from Tophat2 are converted to raw read counts using HTSeq (Anders, Pyl and Huber, 2015). There are many other transcript quantification tools available, such as RSEM (Li and Dewey, 2011) and StringTie (Pertea *et al.*, 2015), which utilize the BAM file generated from Tophat2 and reference GTF file and produce Reads Per Kilobase of transcript per Million (RPKM) reads. HTSeq utilizes a simpler approach and produces raw read count from the SAM file and reference GTF file. Raw reads were then used for DGE using DESeq (Anders and Huber, 2010) and edgeR (Robinson, McCarthy and Smyth, 2010). There are many other tools available for RNA-Seq DGE analysis such as NPEBseq (Bi and Davuluri, 2013), NOISeq (Tarazona *et al.*, 2012), baySeq (Hardcastle and Kelly, 2010), DEGSeq (Wang *et al.*, 2009) and EBSeq (Leng *et al.*, 2013). Cuffdiff was chosen as it is specifically designed for DGE analysis from transcripts, spliced regions and promoters, and is best suited to use in conjunction with TopHat2. Since some of the samples in the study did not contain any replicates, DESeq and edgeR were chosen because both the tools are designed to work with and without replicates. Additionally, coupling HTSeq with DESeq and edgeR helps in direct integration of raw read counts from *htseq-count* as input into DESeq and edgeR programs. Post-analysis was performed using the SpliceR (Vitting-Seerup *et al.*, 2014) tool for annotation of transcript features obtained from Cuffdiff (Trapnell *et al.*, 2012). Results from Cuffdiff, DESeq and edgeR were merged to obtain collective DEGs in the sample pairs. The final step of the pipeline consisted of gene enrichment, pathway analysis and protein-protein interaction (PPI) network analysis using the Araport portal (Krishnakumar *et al.*, 2015), ClueGO (Bindea *et al.*, 2009) and GeneMania (Montojo *et al.*, 2010) for identifying novel gene clusters associated with flower development.

2.2 Sample collection and data preparation

Experiments were conducted by Klepikova et al (Klepikova *et al.*, 2015) where a single *A. thaliana* plant (Col-0) was grown in conditions for preventing crossbreeding. Plants were harvested at 7-16 days old to obtain synchronized plants at different developmental stages, denoted by S7 to S16 respectively. Hand-dissected shoot apical meristems were fixed in two biological replicates using tissues from 15 individuals in each sample. 9-14-day old plants were collected in two replicates for a second independent experiment denoted by S9N to S14N respectively. Sequence reads for each sample were obtained from the NCBI Sequence Read Archive under project ID PRJNA268115. A quality report was generated using the FastQC tool to obtain the statistics of reads (Andrews, 2010). The SRA data was converted to FASTQ format using the 'fastq-dump' tool available in the SRA Toolkit, NCBI (Sayers *et al.*, 2009).

2.3 Read trimming, reference genome mapping and transcript assembly

Adapter trimming and genome mapping represents the pre-processing step, as seen in Fig. 1. First 15 base pairs of the reads were trimmed using Cutadapt to remove adapter sequences and improve the quality of the reads to keep reads with a Q-score greater than or equal to 30 (Martin, 2011). Each sample consists of two reads; therefore, each read was trimmed and a FastQC report was regenerated on the trimmed data to examine the quality and verify that the resultant reads satisfied the criterion. Trimmed reads were mapped to the *A. thaliana* genome (TAIR10) using the TopHat2 aligner (Langmead and Salzberg, 2012; Kim *et al.*, 2013). We ran TopHat2 on both the reads, with the values of the following default parameter changed to suit *A. thaliana*: minimum

intron length (-i) was set to 40, maximum intron length (-I) was set to 5000, segment length was set to 20, segment mismatches was set to 2, no multi-hits (-g=1), minimum normalized depth (F) was set to 0 and minimum anchor length was set to 10 (-a=10). The parameter values are summarized in Table 1. Trimmed reads were also aligned using Bowtie2 with minimum (i) and maximum (I) intron length set to 30 and 5000 respectively. Previously, it was reported in some studies that the minimum functional intron length for monocots and dicots was found to lie between 70 to 73 nucleotides (nt) (Goodall and Filipowicz, 1990). However, certain genome-wide studies performed on *A. thaliana* and *O. sativa* datasets provides evidence of introns shorter than 60 nt with size range of 20 to 59 nt in length (Deutsch and Long, 1999; Wang and Brendel, 2006). Similarly, the maximum intron length for plant genomes, which is otherwise set to 500bp, is much larger than vertebrates. Since each read is cut into segments that are mapped independently, the segment length for shorter reads in our case should be decreased from its default value. By setting the max multihits option to 1, we are forcing unique mapping of the reads to the genome which will allow best mapping of the read to the genome. By setting the value of minimum anchor length to 10 instead of 8, TopHat2 will report junctions spanned by reads with at least this many bases on each side of the junction. Finally, to eliminate the heuristic filter associated with vertebrate genomes, minimum normalized depth was set to 0 instead of 300.

Reads aligned using TopHat2 were then used by Cufflinks (Fig. 1) for assembling individual transcripts with –i 40 and -I 5000 parameters (Trapnell *et al.*, 2012). In plant genomes, the difficulty of estimation of transcript abundance arises due to multi-reads and the genome becomes highly-repetitive. Therefore, to address the uncertainty, an Expectation-Maximization algorithm (EM) has been applied using Cufflinks for estimating transcript abundance which computes fractional distribution of each multi-read after read alignment in the E-step and then estimates relative abundance of transcripts in the M-step until it converges. After obtaining the transcripts for each read, transcripts from two comparable samples were merged using Cuffmerge (Trapnell *et al.*, 2012). For example, for comparing S7 with S8, the transcripts of each read of the two samples which is equal to 4 read transcripts were merged to form an assembled transcript GTF file for further analysis.

2.4 Differential gene expression analysis on time-series apical shoot data

Differential expression analysis of the reads was carried out by testing the samples at day 8 to 16 (S8 to S16) after germination against the sample from day 7 (S7) to obtain DEGs at each consecutive stage. The reason why day 7 was chosen for benchmarking was that plants at this stage after germination had the first and second leaves visible; while on day 16th they had ten visible leaves. Comparisons of two samples from consecutive days were also made (Table 2). These analyses were carried out using Cuffdiff (Trapnell *et al.*, 2012). The multi-read-correct option was enabled to carry out an initial estimation procedure for accurately weighting reads for mapping to multiple locations on the genome. Quartile normalization was used to obtain Fragments Per Kilobase Million (FPKM) and fragment counts via the ratio of 75th quartile fragment counts to 75th quartile value across all samples. False discovery rate (FDR) adjusted p-values (known as q-values) were obtained from the analysis and significantly expressed genes were obtained by filtering q-values less than or equal to 0.05.

Sequence read counts were obtained from the reads aligned by Tophat2 using the HTSeq tool to generate raw read counts (Anders, Pyl and Huber, 2015). The read counts were then used to produce a list of differentially expressed genes using DESeq (Anders and Huber, 2010) and edgeR (Robinson, McCarthy and Smyth, 2010). As in the previous step, comparative analysis of S7 against S8 to S16 and step-wise analysis were conducted. Since the dataset contains partial replicates for 5 samples (S9N to S14N), we used blind dispersion estimation for samples with no replicates along with the sharing mode set to 'fit-only' and we used pooled empirical dispersion for samples with one or more replicates. The negative binomial method was applied for obtaining DEGs. Results were filtered based on FDR <= 0.05 and $\log_2$ fold-change less than -2 and greater than 2. To compare samples involving replicates, the generalized linear model (GLM) was applied for estimating common and tagwise dispersion. To compare samples for which no replicates were found, Fisher's exact test was applied with the biological coefficient of variation set to 0.2 (Benjamini and Hochberg, 1995). For performing DGE analysis using edgeR for samples having no biological replicates, we used common BCV (Biological Coefficient of Variation) with square-root dispersion value which was set to 0.4 for humans and 0.1 for genetically identical organisms.

2.5 Alternative splicing classification analysis using SpliceR

To obtain statistics of transcript level information, we utilized SpliceR (Vitting-Seerup *et al.*, 2014) to classify isoform transcripts obtained from Cuffdiff. Output files containing FPKM tracking, count tracking and read group tracking files enabled us to detect exon skipping/inclusion (ESI) events, alternative transcription start site (ATSS), alternative transcription termination site (ATTS), alternative 3' splice site (A3), alternative 5' splice site (A5) and mutually exclusive exon (MEE) events. Additionally, the average number of transcripts per gene and the average number of ESI events per transcript were computed using the *spliceR* function for each of the "Against S7" and "Step Analysis" sample pairs.

2.6 GO enrichment, pathway and protein-protein interaction analysis

Results obtained from the overlap of Cuffdiff, DESeq and edgeR were used for functional enrichment to categorize genes and their associated functions. Overlapping DEGs had to express more than once in "Against S7" and "Step analysis" results to be retained for further analysis. GO enrichment functional annotation and clustering of the genes were performed using the Araport portal (Krishnakumar *et al.*, 2015) to identify genes associated with enriched categories. Gene identifiers (e.g. AT1G02335) were used as inputs into the Araport Thalemine tool. These identifiers were then used for enrichment in gene ontologies (biological process, cellular component and molecular function). Pathway analysis was performed using the ClueGo plugin (Bindea *et al.*, 2009) of the Cytoscape software (Shannon *et al.*, 2003). Gene identifiers were used to identify the association and clustering of genes in pathways using KEGG (Ogata *et al.*, 1999), REACTOME (Croft *et al.*, 2014) and WikiPathways (Kutmon *et al.*, 2015) databases. Enrichment or depletion of GO categories in ClueGO was performed using the two-sided hypergeometric test and FDR was calculated for the enriched GO categories using the Benjamin and Hochberg approach (Benjamini and Hochberg, 1995). Gene enrichment and clustering results obtained from Araport and Cytoscape were further filtered with FDR <= 0.05 to identify

highly significant enriched clusters. A PPI network was constructed using the GeneMania plugin (Montojo *et al.*, 2010) of the Cytoscape software (Shannon *et al.*, 2003) to obtain prevalent interactors and their degree of interactions from the network.

2.7 Calculation of relative expression values

To calculate relative expression values, FPKM counts were used in each sample pair and counts were normalized by dividing by the sample pair read count by the maximum read count value from all other sample pairs (i.e. S7-S8 to S7-S16) to obtain relative expression value between 0 and 1. Expression profiles of each gene were constructed by comparing expression values from Cuffdiff and DESeq-edgeR.

2.8 Calculating correlation of expression values

For calculating correlation between the expression profiles, Pearson Correlation Coefficient (PCC) was used. Expression profiles of differentially expressed genes involved in flower development were compared against expression profiles of *FLC* and *LFY* genes to obtain PCC between them. Also, difference in expression using PCC was also evaluated by comparing expression profiles of genes obtained from Cuffdiff, DESeq and edgeR with those obtained from Klepikova et al. (Klepikova *et al.*, 2015).

2.9 Data availability

An apical shoot meristem time-series dataset has been deposited by other researchers in the NCNI SRA database under project ID PRJNA268115 (Klepikova *et al.*, 2015) has been used in this study. Analysis pipelines listing the data processing and differential gene expression steps constructed and revealed through our research has been provided as Linux shell scripts which can downloaded from GitHub https://github.com/deshpan4/RNA-Seq-pipeline.

3. Results

3.1 Differential expression analysis of time-series apical shoot data

Results obtained from DGE of five sample pairs were computed in “Against S7” and “Step Analysis” manner as detailed in Table 2. When comparing with S7, 5,266 DEGs were obtained for S7-S10, 2,841 genes for S7-S11, 4,760 for S7-S12, 6,337 for S7-S13 and 2,532 genes for S7-S14 pair. DGE using “Step analysis” was performed to identify genes differentially expressed from the previous day which yielded fewer genes as compared to that obtained from “Against S7” sample pairs.

Next, we studied the overlap between Cuffdiff, DESeq and edgeR for sample pairs in “Against S7” and “Step Analysis”. By overlapping DEGs, 418 genes were found for S7-S10 with FDR <= 0.05. Using the same cutoff, S7-S11 generated 277 genes, S7-S12 produced 520 genes, S7-S13 gave 1,534 genes and S7-S14 gave 150 genes (Table 3). On the other hand, 28 genes were found for S9-S10, 3 genes for S10-S11, 7 genes for S11-S12, 38 genes for S12-S13 and

74 genes were found for S13-S14. Overlapping genes were also found for Cuffdiff-edgeR, DESeq-edgeR and Cuffdiff-edgeR-DESeq pairs (Table 3). From Cuffdiff-DESeq-edgeR overlap, we identified 690 genes in “Against S7” and 19 genes in “Step analysis” which are significantly expressed in more than one sample pair. This set of common genes is referred to as CGenes in the following analysis.

3.2 GO enrichment and pathway analysis of differentially expressed genes in the transition phase

GO enrichment analysis applied to CGenes were classified in three categories: Biological Process (BP), Molecular Function (MF) and Cellular Component (CC). Results from GO enrichment (Fig. 2) of common genes obtained from “Against S7” sample pairs show 664 genes were significantly enriched in BP and CC ontologies with p-values < 0.05. Whereas those obtained from “Step Analysis” sample pairs show 18 genes significantly enriched only in the BP ontology with p-value < 0.05. From the pathway analysis of “Against S7” DEGs, 30 genes have been found to be involved in Glucosinolate Biosynthesis, 2-Oxocarboxylic acid metabolism, Sulfur metabolism, Cysteine and methionine metabolism with FDR ≤ 0.05 whereas for “Step Analysis” only 4 genes were found to be involved in 2-Oxocarboxylic acid metabolism, C5-Branched dibasic acid metabolism, Valine, leucine and isoleucine biosynthesis.

Additionally, pathway analysis using ClueGo revealed 33 genes associated with 8 GO terms which were found specifically in KEGG and REACTOME (Table 4). Pathway enrichment of 19 common genes from “Step Analysis” sample pairs shows association of *BCAT4*, *IMD1* and *IPMI2* genes in the valine, leucine and isoleucine biosynthesis pathways with significant term p-value < 0.05.

3.3 Analysis of expression profiles of enriched genes involved in glucosinolate biosynthesis and metabolism

Expression profiles were constructed from the set of enriched genes by selecting the highly enriched cluster from the CGenes set. Fig. 3 shows the relative expression profiles of the genes expressed in “Against S7” and “Step analysis” sample pairs that play major roles in Glucosinolate Biosynthesis (GluBP), Glycosinolate Biosynthesis (GlyBP), Glucosinolate Metabolic Process (GluMP), Glycosinolate Metabolic Process (GlyMP), Sulfur-Compound Biosynthetic Process (SCBP) and Sulfur-Compound Metabolic Process (SCMP). 21 genes have been found to be associated with GluBP and GlyBP, 27 associated with GluMP and GlyMP, 25 associated with SCBP and 37 have been found to be associated with SCMP. From the expression profiles expression of the genes peaks at S7-S8 and S7-S9 pairs in “Against S7”. The expression decreases to 0.4 in S7-S10. It continues to decrease until it reaches 0 in S7-S13 and continues for the rest of the samples for most of the genes. It is clearly visible that *ACO1*, *ACO2*, *APS1* and *AT4G05090* display different behavior where expression varies between 1 and 0.6 for SCMP. In SCBP, *CYSD1* expression value remains constant between 0.6 and 0.8 whereas for *CYP83B1* value suddenly increases from 0.4 in S7-S12 to 0.9 in S7-S13, drops to 0.4 in S7-S14 and again increases to 0.9 in S7-S15 and S7-S16. In GBP, only *CYP83B1* shows variable expression. Apart from these genes, certain other genes such as *TGG1* and *TGG2* show a “zig-zag” expression pattern which encodes myrosinase enzymes and helps in the breakdown of glucosinolates (Barth

and Jander, 2006). As compared to these genes, *CYP83B1* and *CYP83A1* are expressed in the SCMP, SCBP and GluBP. These encode non-redundant enzymes which also metabolize oximes in glucosinolate biosynthesis (Naur *et al.*, 2003). Where the expression of *CYP83A1* follows a general curve of steep decrease in expression from S7-S9, expression of *CYP83B1* is non-identical and shows a "zig-zag" expression pattern like *TGG1* and *TGG2*. Similarly, *ACO1* and *ACO2* in the SCMP also differ in their expression profiles despite being similar in structure and function. *CYP79B3* also encodes a cytochrome protein however its expression is dissimilar from *CYP83B1* which can be clearly distinguished in the GluBP where the value starts to decrease from S7-S8 to S7-S14 and increases from 0.08 to 0.43 in S7-S16.

3.4 Expression profiles of differentially expressed flowering genes

From CGenes, genes responsible for flowering and involved in regulation of flower development were identified. 5 genes were found to be involved in "Flowering". 18 were found to be associated with "Flower Development", 8 with "Regulation of Flower Development" and 3 with "Negative Regulation of Flower Development". Fig. 4 shows expression profiles of genes involved in flowering, flower development, regulation of flower development and negative regulation of flower development. In "Against S7" sample pairs, many experimental genes such as *FLC*, *SOC1*, *EMS1* and *FD* have also been identified by enrichment analysis. Expression profiles of flowering genes shows that *SOC1*, *FCA*, *SAP* and *AGL31* increase in expression as compared to *FLC* which decreases in expression in "Against S7". All four genes show increase in expression in S7-S10 which is followed by decrease in expression in S7-S11. *FCA*, *SAP* and *SOC1* show highest expression in S7-S14 whereas the expression for *AGL31* remains constant between 0.2 and 0.4 and finally increases to 1 in S7-S16. In the "Flower Development" process, a large cluster of genes in "Against S7" sample pairs display a "zig-zag" pattern of expression. There are four gene clusters observed in this process. The first cluster consists of *ATX1*, *RDR6*, *SOC1*, *KAN2*, *BPE*, *SRS2*, *FCA*, the expression values of which increase in S7-S9, decrease in S7-S11 and increase again in S7-S12. The second cluster consists of *ATX1*, *NAC054*, *NGA1* and *F-ATMBP* shows a decrease in expression followed by an increase in S7-S15 and S16. The third cluster consists of *EMS1*, *KAN2*, *ABCB19*, *SOC1* and *SAP1* shows a peak in expression value from S7-S14. The fourth cluster of genes consists of *SPT*, *SRS2*, *ATX1* and *FCA* in S7-S14 where the expression varies between 0.7 and 0.8. In the "Regulation of Flower Development" process, *POLA*, *FD*, *ATX1*, *SOC1*, *AGL31* and *FCA* show a decrease in expression in S7-S11 whereas *ATX1* shows an increase in expression in S7-S11. In the "Negative Regulation of Flower Development" process, only *FLC*, *AGL31* and *POLA* are expressed. It is important to note that *FLC* has been found to be involved in all the processes of flowering, flower development, regulation and negative regulation of flower development.

3.5 Identifying important regulators using protein-protein interaction (PPI) network analysis

Interactions between DEGs were studied for identifying most prevalent interacting genes and their regulation on neighboring genes. PPI network was constructed for identifying highly connected genes and their most prevalent interactions (Figure 5a). From PPI network analysis, 18 genes were found to have highest interactions with edges ≥ 100 and significantly involved in Glucosinolate Biosynthesis. PPI network analysis revealed that along with 18 genes, 114 genes

(Figure 5b) were involved in induced systemic resistance, sulphur compound biosynthetic process, cellular biogenic amine metabolic process, sulphur metabolism and biosynthesis, anion transport, organic acid transport and cellular response to external stimulus.

3.6 Identification of floral candidate genes

FPKM expression values of *FLC* and *LFY* genes from Day-1 to 10 were used to identify potential novel genes from the CGenes set by selecting those displaying the highest correlation with *FLC* and *LFY* expression profiles and having no ontology information for *A. thaliana*. Results of correlation and GO enrichment analysis using Araport (Krishnakumar *et al.*, 2015) showed that 69 and 7 genes which displayed the highest correlation (PCC≥0.9) in expression to *FLC* and *LFY* respectively did not get enriched in any biological or molecular function (Fig. 6). These genes were labeled as novel genes which can regulate the expression of other known floral regulators during the flowering transition phase. For identification of genes regulated by *FLC* or *LFY*, node connections were studied by filtering out genes connected with *FLC* or *LFY*. Table 5 lists genes regulated and not regulated by *FLC* and *LFY* genes. 69 genes were found to be highly correlated by *FLC* out of which 14 genes were regulated and 55 genes were non-regulated. Similarly, for *LFY*, out of 7 genes 4 were regulated and 3 were non-regulated in the PPI network.

3.7 Identification of alternative splicing classes in transcripts

From the SpliceR analysis, we identified 1.23 transcripts per gene in the S7 sample and approximately 1.27 transcripts for each sample compared against S7 in the “Against S7” sample pairs, whereas 2.27 and 2.26 transcripts per gene were observed for the “Step analysis” sample pairs. Looking at ESI-AS events in “Against S7”, we observed 0.1 ESI events per gene for S7 and 0.07 for each compared sample, whereas in the “Step analysis” sample pairs, 0.08 ESI events per gene were observed for both samples.

4. Discussion

Recent progress in determination of DGE in RNA-Seq data using several bioinformatics tools enabled easier identification of genes from samples. A number of tools for processing and analysing RNA-Seq data have been developed. These include Cufflinks, edgeR, DESeq, RSEM and others which claimaccurate identification of DEGs. However, the accuracy can only be determined by comparison of results obtained from several computational tools with those obtained from published experimental studies. Using recently published tools for RNA-Seq data, a comparative analysis of results obtained from Cufflinks-Cuffdiff2, DESeq and edgeR was performed and analysis of intersection of DEGs from two or more tools was recommended in order to obtain more robust results (Zhang *et al.*, 2014). In the current study, we have proposed an approach for the identification of DEGs in *A. thaliana* RNA-Seq time-series datasets which includes quality checking, adapter trimming, reference alignment, DEG analysis, alternative splicing classification, DEG merging, GO enrichment and pathway analysis (Fig. 1). The first step in identification of DEGs is to perform accurate genome alignment. Inaccurate parameters often result in the generation of incorrect read counts from the data which could potentially result in

erroneous downstream processing. Previous investigations indicated use of default values for processing RNA-Seq data (Klepikova *et al.*, 2015) which included similar minimum intron length values of 70 nt for plants and mammals (Goodall and Filipowicz, 1990). However, mean, medium and minimum intron length in *A. thaliana* and *O. sativa* was found to be much lower (Deutsch and Long, 1999; Wang and Brendel, 2006) than the previously identified and established value of 70 nt. Therefore, to correctly identify DEGs from the data, custom parameter values were applied to generate precise alignment of samples against the reference genome. The pipeline was specifically focused on accurate processing and analysis of A. thaliana time-series datasets with application in flower development. The analysis was performed by comparing S7 with other samples in a way that S7 was treated as case and the comparing sample was treated as control to identify DEGs. Additionally, analysis was also performed by progressively analyzing the case-control samples in a stepwise manner (Table 2).

4.1 Known floral transition related genes and their interactions

In *A. thaliana* the transition to flowering is controlled through the regulation of certain genes of which FLC and LFY are the most important (Deng *et al.*, 2011; Siriwardana and Lamb, 2012). The transition process involves interaction of FLC with key genes such as *SUPPRESSOR OF OVEREXPRESSSON OF CONSTANS 1* (SOC1), *FLOWERING LOCUS T* (FT) and *FLOWERING LOCUS D* (FLD) (Deng *et al.*, 2011). However, other repressors such as *TERMINAL FLOWER1* (TFL1), *SHORT VEGETATIVE PHASE* (SVP), *TARGET OF EAT1/2* (TOE1/2), *MADS AFFECTING FLOWERING1* (MAF1) to MAF5, *EMBRYONIC FLOWER1* (EMF1) and EMF2 have also been found to be involved for regulation of flowering time (Hartmann *et al.*, 2000; Piñeiro *et al.*, 2003; Ratcliffe *et al.*, 2003; Mathieu *et al.*, 2009; Hanano and Goto, 2011; Zhang *et al.*, 2015). *FLC* in particular binds to more than 500 target sites in the Arabidopsis genome and regulates genes which function in developmental pathways (Deng *et al.*, 2011). One of the known interactions of *FLC* is with *FRIGADA* (FRI) where both the genes interact to control flowering time (Caicedo *et al.*, 2004). Expression of *FLC* is also regulated by PHD-polycomb repressive complex 2 (PRC2) consisting of *VRN2*, Su(z)12 homologue and PHD finger proteins VIN3 and VRN5. Repression of *FLC* is mediated by cold-induced epigenetic silencing mechanism during vernalization (De Lucia *et al.*, 2008). Like *FLC*, expression of *SVP* is controlled by the trithorax (TrxG) protein called *BRAHMA* (BRM) (Li *et al.*, 2015). Similarly, the *EARLY BOLTING IN SHORT DAYS* (EBS) protein participates in flowering time regulation by repressing the *FT* protein and *CURLY LEAF* (CLF) protein represses the expression of *AGAMOUS LIKE* (AGL) genes (Piñeiro *et al.*, 2003).

On the other hand, *LFY* acts as a positive regulator of *APETALA1* (AP1) and the expression of *AP1* was observed late during photo-induction when examined during light treatments (Hempel *et al.*, 1997). During shoot development, members of the *SQUAMOSA PROMOTER BINDING PROTEIN-LIKE* (SPL) transcription factor family genes viz, *SPL9* and *SPL15* have been known to control shoot maturation (Schwarz *et al.*, 2008). Llike *LFY,* which is a floral meristem identity protein, *CAULIFLOWER* (CAL), *FRUITFUL* (FUL), *AGAMOUS LIKE24* (AGL24), SEP MADS box transcription factors SEP3/4 and *LATE MERISTEM IDENTITY1/2* (LMI1/2) are also floral meristem identity proteins in Arabidopsis (Kempin, Savidge and Yanofsky, 1995; Ferrándiz *et al.*, 2000; Ditta *et al.*, 2004; Castillejo, Romera-Branchat and Pelaz, 2005;

Saddic *et al.*, 2006; Gregis *et al.*, 2008; Pastore *et al.*, 2011; Siriwardana and Lamb, 2012). Flowering during long days is also mediated by regulation of certain proteins. The transcription factor CONSTANS (CO) plays a major role in the long-day pathway as this protein is phosphorylated. Therefore it plays a major role in the abundance of the protein (Zhang *et al.*, 2015). Phosphorylated CO is preferentially degraded when CONSTITUTIVE PHOTOMORPHOGENIC 1 (COP1) ubiquitin ligase complex is activated (Sarid-Krebs *et al.*, 2015). Furthermore, COP1 protein has also been known to interact with the Arabidopsis cryptochromes (CRY1 and CRY2) through C-terminal domains (CCT) (Yang, Tang and Cashmore, 2001). During floral transition certain genes such as *FLOWERING PROMOTIVE FACTOR1* (*FPF1*) are expressed in apical meristems and are involved in the GA-dependent signaling pathway which regulates the GA response in apical meristem (Kania *et al.*, 1997).

4.2 Overlapping of Cuffdiff with DESeq and edgeR genes

The key step of RNA-Seq data analysis is to identify DEGs using appropriate statistical models. Once the FPKM counts from the sequencing reads were obtained, these were used for finding DEGs using Cuffdiff, DESeq and edgeR. The statistical model in Cuffdiff which is used to evaluate the changes in expression assumes that the number of reads produced by each transcript is proportional to its abundance, although it fluctuates because of biological variability between the replicates and technical variability during sequencing and library preparation. DESeq, on the other hand, allows the user to supply multiple as well as no replicates. DESeq is highly useful when no replicates are present in the datasets. The statistical model in DESeq uses a blind dispersion method that is particularly useful with no replicates where the outlier values cannot be captured during dispersion estimation. On the other hand, edgeR uses both the generalized linear model (glm) and classical empirical Bayes methods, which are used for estimation of gene-specific biological variations even with those datasets having a minimal level of biological variations. Usage of Cuffdiff, DESeq and edgeR methods increase statistical power and help in rationale comparison and thus confirming the suitability of the results. Therefore, DE analysis has been carried out for further comparison in the present investigation.

Results show that both Cuffdiff and edgeR displayed significant numbers of differentially expressed genes in S7-S10, S7-S12 and S7-S13 (Table 3). Overlapping of genes can be visualized by Venn diagrams constructed for transition phase samples (Fig. 7). We see in Fig. 7 the intersection of Cuffdiff-DESeq-edgeR, Cuffdiff-DESeq and Cuffdiff-edgeR decreases in “Step analysis” sample pairs as compared to “Against S7” sample pairs. edgeR additionally displayed a greater number of DE genes in S7-S14, S7-S15 and S7-S16 which are not notably identified by Cuffdiff or edgeR. On the contrary, Cuffdiff displays the maximum number of DE genes from “Step analysis” results as compared to DESeq and edgeR. By comparing the results of Cuffdiff with DESeq and edgeR, we clearly observed that the overlap from Cuffdiff-edgeR was more significant than Cuffdiff-DESeq or DESeq-edgeR. This difference can be clearly observed in “Step analysis” for S10-S11 (Fig. 7g) where 1347 genes were found to be common for Cuffdiff-edgeR as compared to 4 for Cuffdiff-DESeq. Thus, the total number of common genes was significantly reduced for Cuffdiff-DESeq-edgeR intersection which is primarily due to a smaller gene count in Cuffdiff-DESeq. Thus only 1% of the genes were found to be common for Cuffdiff-DESeq-edgeR

confirming that the decrease in the overlap is mostly due to DESeq results. A significant number of genes were found to have an overlap in S7-S13 pairs as shown in Fig. 7d.

4.3 Comparison of profiles of differentially expressed genes

FLC and *LFY* are the two most important genes which regulates transition to flowering and are widely known to play major role in flower development. Using PCC metric, we evaluated similarity in expression profiles of FLC and LFY obtained in this study and compared with profiles obtained from Klepikova et al (Klepikova *et al.*, 2015). Consistent with the experimental findings, our results as shown in Fig. 8 (a, b, c and d) displays higher mean PCC of 0.86 and 0.88 for *FLC* and *LFY*, respectively which is consistent with published results (Michaels, 1999; Klepikova *et al.*, 2015). From our results, *SVP* has been shown to be highly expressed in all samples during the transition phase which was consistent with the results from Klepikova et al. *SOC1,* on the other hand, showed a five-fold increase in expression during S7 to S10. Contrary to these results from Klepikova et al., our results showed consistently higher expression of *SOC1* in transition phase samples from S7 to S14. Similarly, where the expression of *FLD* showed increase in later stages of floral induction (Klepikova *et al.*, 2015), expression of *FLD* has been found to be consistently higher in all the stages of flower development in our results. However, we found correlation in expression patterns of genes from the *SPL* gene family between our results and those of the results of Klepikova et al. and others. . *SPL3*, *SPL4* and *SPL5* showed decrease in expression whereas *SPL9* and *SPL15* showed increase in expression which was consistent with published results (Schwarz *et al.*, 2008). In "Against S7" sample pairs, expression of *AP1* showed increase in late transition phase stages (i.e S13 and S14) consistent with Hempel et al. (Hempel *et al.*, 1997) and Ferrándiz et al. (Ferrándiz *et al.*, 2000) whereas expression of *AP1* was observed in S14 only (Klepikova *et al.*, 2015). Experimental results show COP1 interact with CRY1 and CRY2 proteins in apical shoots (Yang, Tang and Cashmore, 2001; Sarid-Krebs *et al.*, 2015). Additionally, increased expression of *FPF1* (from Cuffdiff and edgeR) has also been observed in our results which is consistent with the published results during the transition phase (Kania *et al.*, 1997). Expression profiles of *FPF1*, *SPL9* and *SPL15* have found to be correlated with *LFY* expression (Fig. 8b, d, e and f).

Expression of experimental genes were roughly categorized into 4 different types, namely, (1) genes similar in expression to *FLC* displaying decrease in expression from S7-S8 to S7-S16 and S15-S16, (2) genes displaying increase in expression from S7-S8 to S7-S16 and S15-S16, (3) genes having variable expression between 1 and 0.6, and (4) genes showing increase in expression followed by a decrease in expression. Genes displaying higher PCC to *FLC* are *SNZ*, *SMZ*, *TOE2* and those having higher PCC to *LFY* are *FPF1*, *CAL*, *AP1*, *SOC1*, *SPL9*, *SPL15*, *EMF2*, *CO*, *AGL71*, *MAF2* and *MAF3*. Genes having lower PCC are *LHP1*, *EMF1*, *EBS*, *VRN2*, *CRY1*, *LD*, *FRI*, *FIE*, *FLD*, *BRM*, *COP1*, *CLF*, *SVP*, *PHYB*, *MAF1*, *CRY2*, *MAF4* and *MAF5*. *TFL1* showed increase in expression in S7-S14 whereas *FT* showed increase in expression in S7-S11 which was followed by sudden drop in expression values for both *TFL1* and *FT*.

4.4 Comparison of expression profiles of cell-cycle related genes

Expression patterns of cyclin dependent kinases (CDKs) obtained from the pipeline were also compared to obtain degree of variation between those obtained from Klepikova et al. (Klepikova

et al., 2015) which included CDKA, CDKB, CDKC, CDKD, CDKP, CDPT and cyclin genes. Results from the comparison shows that most of the CDK genes exhibited moderate correlation with an average ranging between 0.60 – 0.70. While some of the CDKs such as *CYCA3;4*, *CYCB1;1*, *CYCC1;2*, *CYCD1;1*, *CYCD2;1*, *CYCD6;1*, *CYCD4;2*, *CYCP3;1*, *CYCP3;2*, *CDKE;1*, *CDT1A*, *CYCJ18*, *CYL1* and *CYCH;1* displayed particularly higher correlation above 0.90, some displayed particularly poor correlation which included *CKS1*, *CDKB1;1*, *CDKB1;2*, *CDKA;1/CBC2*, *CYCA1;1*, *CYCB3;1*, *CYCB1;5*, *CYCB1;2/CYC1BAT*, *CYCC1;1*, *CYCD4;1*, *CYCP4;1*, *CYCT1;4*, *CDKD;3/CDKD1;3*, *CDKD;1/CDKD1;1* and *CYCL1/RCY1* ranging between 0.20 – 0.60. Correlation analysis shows that some of the cyclin genes exhibit greater similarity, whereas the majority of CDKB and CDKD genes exhibits greater dissimilarity. Expression profiles of poorly correlated genes such as CKS1 obtained from Klepikova et al. shows single peak at M5 (Day-11) whereas two peaks were found on Day-9 and Day-12 in samples S7-S9 and S7-S12. Experimental results clearly show that CKS1 was constitutively expressed during mitotic and endoreduplication cycles (Jacqmard *et al.*, 1999). This supports the hypothesis that the gene should be highly expressed during the flowering transition phase. Similarly, *CDKB1;1* has also been found to be highly expressed in shoot meristem in *A. thaliana* (Skylar, Matsuwaka and Wu, 2013) which supports the evidence of multiple peaks observed in our results.

4.5 Protein-protein interaction network analysis of differentially expressed genes

Results of PPI network analysis shows most of the DEGs during the transition phase regulate other DEGs which provide induced resistance and protection against external factors such as stress, pathogens, herbivores, temperature variations, etc. A recent study on the relationship of glucosinolates to flowering in *A. thaliana* suggests that presence of the *MAM1* gene affects glucosinolate accumulation and flowering time in the absence of *APOP2* and *APOP3* genes and leads to production of C3 glucosinolates (Jensen *et al.*, 2015). Results from the PPI network analysis clearly show that *MAM1* regulates several other genes in glucosinolates and displays a high expression profile correlation of 0.75 to *FLC* which supports the hypothesis of glucosinolate production and protection during flowering phase. Glucosinolates are sulphur and nitrogen-rich chemical compounds in plants that provide defense against pathogens and herbivores by forming a toxic compound upon herbivore attack when the cell wall is ruptured (Jensen *et al.*, 2015; Mohammadin *et al.*, 2017). Glucosinolates play a crucial role in flowering time regulation during transition from vegetative to reproductive phase and also provide protection from herbivores and pathogens for the plant's vegetative and generative tissues during the transition phase. Therefore, differential expression of glucosinolates during the transition phase becomes essential.

We also identified genes responsible for flowering and involved in flowering and in regulation of flower development from the clustering of 690 expressed genes. Expression profiles of these associated genes were constructed to observe similarities and differences among profiles of experimental genes (Fig. 4). *SPT1*, *RDR6*, *SRS2*, *SAP*, *SOC1* clearly showed increase in expression at S12-S13 in "Flower Development" whereas it showed a "zig-zag" pattern of expression in "Against S7". In contrast, genes such as *NGA1* and *NAC054* displayed a decrease in expression from 0.5 in S7-S13 to 0.1 in S7-S14 and a sudden increase to 1 in S7-S16. Genes such as *SOC1* and *F-ATMBP* showed an increase in expression. Expression profiles of genes in "Step Analysis" showed a distinct peak at S12-S13 which strongly indicates that genes associated

with flowering and flower development show identical expression profiles and are expressed only during transition phase.

Conclusions

In this study, we conducted rigorous investigation and analysis of apical shoot meristem time-series dataset obtained from *A. thaliana*. We constructed a pipeline for identification of differentially expressed genes from overlap of three tools and identified 690 genes. Their functional enrichment was conducted for identification of genes associated with highly enriched biological processes. We also constructed expression profiles of genes enriched in flowering and in the regulation of flower development. We observed that some of these genes displayed distinct expression profiles when compared to those displayed by already known experimental genes which are commonly regulated during floral transition. Additionally, PPI network analysis was conducted to identify prevalent interactors and associated functions during the transition phase. 76 novel genes were identified as showing stronger regulation in the network and displaying the highest correlation in expression with *FLC* and *LFY* genes. Further experiments will validate and confirm gene regulation and specific PPIs of the novel genes obtained from the current analysis.

References

Anders, S. and Huber, W. (2010) 'Differential expression analysis for sequence count data.', *Genome biology*, 11(10), p. R106. doi: 10.1186/gb-2010-11-10-r106.

Anders, S., Pyl, P. T. and Huber, W. (2015) 'HTSeq-A Python framework to work with high-throughput sequencing data', *Bioinformatics*, 31(2), pp. 166–169. doi: 10.1093/bioinformatics/btu638.

Andrews, S. (2010) *FastQC: A quality control tool for high throughput sequence data.*, *http://www.bioinformatics.babraham.ac.uk/projects/fastqc/*. doi: citeulike-article-id:11583827.

Barth, C. and Jander, G. (2006) 'Arabidopsis myrosinases TGG1 and TGG2 have redundant function in glucosinolate breakdown and insect defense', *Plant Journal*, 46(4), pp. 549–562. doi: 10.1111/j.1365-313X.2006.02716.x.

Benjamini, Y. and Hochberg, Y. (1995) 'Controlling the false discovery rate: a practical and powerful approach to multiple testing', *Journal of the Royal Statistical Society*, pp. 289–300. doi: 10.2307/2346101.

Bi, Y. and Davuluri, R. V (2013) 'NPEBseq: nonparametric empirical bayesian-based procedure for differential expression analysis of RNA-seq data.', *BMC bioinformatics*, 14(1), p. 262. doi: 10.1186/1471-2105-14-262.

Bindea, G., Mlecnik, B., Hackl, H., Charoentong, P., Tosolini, M., Kirilovsky, A., Fridman, W. H., Pagès, F., Trajanoski, Z. and Galon, J. (2009) 'ClueGO: A Cytoscape plug-in to decipher functionally grouped gene ontology and pathway annotation networks', *Bioinformatics*, 25(8), pp. 1091–1093. doi: 10.1093/bioinformatics/btp101.

Caicedo, A. L., Stinchcombe, J. R., Olsen, K. M., Schmitt, J. and Purugganan, M. D. (2004) 'Epistatic interaction between Arabidopsis FRI and FLC flowering time genes generates a

latitudinal cline in a life history trait.', *Proceedings of the National Academy of Sciences of the United States of America*, 101(44), pp. 15670–5. doi: 10.1073/pnas.0406232101.

Castillejo, C., Romera-Branchat, M. and Pelaz, S. (2005) 'A new role of the Arabidopsis SEPALLATA3 gene revealed by its constitutive expression', *Plant Journal*, 43(4), pp. 586–596. doi: 10.1111/j.1365-313X.2005.02476.x.

Croft, D., Mundo, A. F., Haw, R., Milacic, M., Weiser, J., Wu, G., Caudy, M., Garapati, P., Gillespie, M., Kamdar, M. R., Jassal, B., Jupe, S., Matthews, L., May, B., Palatnik, S., Rothfels, K., Shamovsky, V., Song, H., Williams, M., Birney, E., Hermjakob, H., Stein, L. and D'Eustachio, P. (2014) 'The Reactome pathway knowledgebase', *Nucleic Acids Research*, 42(D1). doi: 10.1093/nar/gkt1102.

Deng, W., Ying, H., Helliwell, C. A., Taylor, J. M., Peacock, W. J. and Dennis, E. S. (2011) 'FLOWERING LOCUS C (FLC) regulates development pathways throughout the life cycle of Arabidopsis.', *Proceedings of the National Academy of Sciences of the United States of America*, 108(16), pp. 6680–6685. doi: 10.1073/pnas.1103175108.

Deutsch, M. and Long, M. (1999) 'Intron-exon structures of eukaryotic model organisms', *Nucleic Acids Research*, 27(15), pp. 3219–3228. doi: 10.1093/nar/27.15.3219.

Ditta, G., Pinyopich, A., Robles, P., Pelaz, S. and Yanofsky, M. F. (2004) 'The SEP4 gene of Arabidopsis thaliana functions in floral organ and meristem identity', *Current Biology*, 14(21), pp. 1935–1940. doi: 10.1016/j.cub.2004.10.028.

Ferrándiz, C., Gu, Q., Martienssen, R. and Yanofsky, M. F. (2000) 'Redundant regulation of meristem identity and plant architecture by FRUITFULL, APETALA1 and CAULIFLOWER.', *Development (Cambridge, England)*, 127(4), pp. 725–734. doi: 10.1046/j.1365-313x.1999.00442.x.

Goodall, G. J. and Filipowicz, W. (1990) 'The minimum functional length of pre-mRNA introns in monocots and dicots', *Plant Molecular Biology*, 14(5), pp. 727–733. doi: 10.1007/BF00016505.

Gregis, V., Sessa, A., Colombo, L. and Kater, M. M. (2008) 'AGAMOUS-LIKE24 and SHORT VEGETATIVE PHASE determine floral meristem identity in Arabidopsis', *Plant Journal*, 56(6), pp. 891–902. doi: 10.1111/j.1365-313X.2008.03648.x.

Gupta, V., Estrada, A. D., Blakley, I., Reid, R., Patel, K., Meyer, M. D., Andersen, S. U., Brown, A. F., Lila, M. A. and Loraine, A. E. (2015) 'RNA-Seq analysis and annotation of a draft blueberry genome assembly identifies candidate genes involved in fruit ripening, biosynthesis of bioactive compounds, and stage-specific alternative splicing.', *GigaScience*, 4(1), p. 5. doi: 10.1186/s13742-015-0046-9.

Hanano, S. and Goto, K. (2011) 'Arabidopsis TERMINAL FLOWER1 is involved in the regulation of flowering time and inflorescence development through transcriptional repression.', *The Plant cell*, 23(9), pp. 3172–84. doi: 10.1105/tpc.111.088641.

Hardcastle, T. J. and Kelly, K. A. (2010) 'baySeq: empirical Bayesian methods for identifying differential expression in sequence count data.', *BMC bioinformatics*, 11(1), p. 422. doi: 10.1186/1471-2105-11-422.

Hartmann, U., Höhmann, S., Nettesheim, K., Wisman, E., Saedler, H. and Huijser, P. (2000) 'Molecular cloning of SVP: A negative regulator of the floral transition in Arabidopsis', *Plant*

Journal, 21(4), pp. 351–360. doi: 10.1046/j.1365-313X.2000.00682.x.

Hempel, F. D., Weigel, D., Mandel, M. a, Ditta, G., Zambryski, P. C., Feldman, L. J. and Yanofsky, M. F. (1997) 'Floral determination and expression of floral regulatory genes in Arabidopsis.', *Development (Cambridge, England)*, 124(19), pp. 3845–3853.

Jacqmard, A., De Veylder, L., Segers, G., De Almeida Engler, J., Bernier, G., Van Montagu, M. and Inze, D. (1999) 'Expression of CKS1At in Arabidopsis thaliana indicates a role for the protein in both the mitotic and the endoreduplication cycle', *Planta*, 207(4), pp. 496–504. doi: 10.1007/s004250050509.

Jensen, L. M., Jepsen, H. S. K., Halkier, B. A., Kliebenstein, D. J. and Burow, M. (2015) 'Natural variation in cross-talk between glucosinolates and onset of flowering in Arabidopsis', *Frontiers in Plant Science*, 6(SEPTEMBER), p. 697. doi: 10.3389/fpls.2015.00697.

Kania, T., Russenberger, D., Peng, S., Apel, K. and Melzer, S. (1997) 'FPF1 promotes flowering in Arabidopsis.', *The Plant cell*, 9(8), pp. 1327–38. doi: 10.1105/tpc.9.8.1327.

Kempin, S. a, Savidge, B. and Yanofsky, M. F. (1995) 'Molecular basis of the cauliflower phenotype in Arabidopsis.', *Science (New York, N.Y.)*, 267(5197), pp. 522–525. doi: 10.1126/science.7824951.

Kim, D., Pertea, G., Trapnell, C., Pimentel, H., Kelley, R. and Salzberg, S. L. (2013) 'TopHat2: accurate alignment of transcriptomes in the presence of insertions, deletions and gene fusions.', *Genome biology*, 14(4), p. R36. doi: 10.1186/gb-2013-14-4-r36.

Klepikova, A. V, Logacheva, M. D., Dmitriev, S. E. and Penin, A. A. (2015) 'RNA-seq analysis of an apical meristem time series reveals a critical point in Arabidopsis thaliana flower initiation', *BMC Genomics*, 16. doi: 10.1186/s12864-015-1688-9.

Koornneef, M., Hanhart, C. J. and van der Veen, J. H. (1991) 'A genetic and physiological analysis of late flowering mutants in Arabidopsis thaliana.', *Molecular & general genetics : MGG*, 229(1), pp. 57–66. doi: 10.1007/BF00264213.

Krishnakumar, V., Hanlon, M. R., Contrino, S., Ferlanti, E. S., Karamycheva, S., Kim, M., Rosen, B. D., Cheng, C. Y., Moreira, W., Mock, S. A., Stubbs, J., Sullivan, J. M., Krampis, K., Miller, J. R., Micklem, G., Vaughn, M. and Town, C. D. (2015) 'Araport: The Arabidopsis Information Portal', *Nucleic Acids Research*, 43(D1), pp. D1003–D1009. doi: 10.1093/nar/gku1200.

Kutmon, M., Riutta, A., Nunes, N., Hanspers, K., Willighagen, E. L., Bohler, A., Mélius, J., Waagmeester, A., Sinha, S. R., Miller, R., Coort, S. L., Cirillo, E., Smeets, B., Evelo, C. T. and Pico, A. R. (2015) 'WikiPathways: capturing the full diversity of pathway knowledge', *Nucleic Acids Research*, 44(October 2015), p. gkv1024. doi: 10.1093/nar/gkv1024.

Langmead, B. and Salzberg, S. L. (2012) 'Fast gapped-read alignment with Bowtie 2', *Nat Methods*, 9(4), pp. 357–359. doi: 10.1038/nmeth.1923.

Leng, N., Dawson, J. A., Thomson, J. A., Ruotti, V., Rissman, A. I., Smits, B. M. G., Haag, J. D., Gould, M. N., Stewart, R. M. and Kendziorski, C. (2013) 'EBSeq: An empirical Bayes hierarchical model for inference in RNA-seq experiments', *Bioinformatics*, 29(8), pp. 1035–1043. doi: 10.1093/bioinformatics/btt087.

Li, B. and Dewey, C. N. (2011) 'RSEM: accurate transcript quantification from RNA-Seq data with or without a reference genome.', *BMC bioinformatics*, 12(1), p. 323. doi: 10.1186/1471-2105-12-323.

Li, C., Chen, C., Gao, L., Yang, S., Nguyen, V., Shi, X., Siminovitch, K., Kohalmi, S. E., Huang, S., Wu, K., Chen, X. and Cui, Y. (2015) 'The Arabidopsis SWI2/SNF2 Chromatin Remodeler BRAHMA Regulates Polycomb Function during Vegetative Development and Directly Activates the Flowering Repressor Gene SVP', *PLoS Genetics*, 11(1). doi: 10.1371/journal.pgen.1004944.

Liu, R., Loraine, A. E. and Dickerson, J. A. (2014) 'Comparisons of computational methods for differential alternative splicing detection using RNA-seq in plant systems.', *BMC bioinformatics*, 15(1), p. 364. doi: 10.1186/s12859-014-0364-4.

De Lucia, F., Crevillen, P., Jones, A. M. E., Greb, T. and Dean, C. (2008) 'A PHD-polycomb repressive complex 2 triggers the epigenetic silencing of FLC during vernalization.', *Proceedings of the National Academy of Sciences of the United States of America*, 105(44), pp. 16831–16836. doi: 10.1073/pnas.0808687105.

Martin, M. (2011) 'Cutadapt removes adapter sequences from high-throughput sequencing reads', *EMBnet.journal*, 17(1), p. 10. doi: 10.14806/ej.17.1.200.

Mathieu, J., Yant, L. J., Mürdter, F., Küttner, F. and Schmid, M. (2009) 'Repression of flowering by the miR172 target SMZ', *PLoS Biology*, 7(7). doi: 10.1371/journal.pbio.1000148.

Michaels, S. D. (1999) 'FLOWERING LOCUS C Encodes a Novel MADS Domain Protein That Acts as a Repressor of Flowering', *THE PLANT CELL ONLINE*, 11(5), pp. 949–956. doi: 10.1105/tpc.11.5.949.

Mohammadin, S., Nguyen, T.-P., van Weij, M. S., Reichelt, M. and Schranz, M. E. (2017) 'Flowering Locus C (FLC) Is a Potential Major Regulator of Glucosinolate Content across Developmental Stages of Aethionema arabicum (Brassicaceae)', *Frontiers in Plant Science*, 8. doi: 10.3389/fpls.2017.00876.

Montojo, J., Zuberi, K., Rodriguez, H., Kazi, F., Wright, G., Donaldson, S. L., Morris, Q. and Bader, G. D. (2010) 'GeneMANIA cytoscape plugin: Fast gene function predictions on the desktop', *Bioinformatics*, 26(22), pp. 2927–2928. doi: 10.1093/bioinformatics/btq562.

Naur, P., Petersen, B. L., Mikkelsen, M. D., Bak, S., Rasmussen, H., Olsen, C. E. and Halkier, B. A. (2003) 'CYP83A1 and CYP83B1, two nonredundant cytochrome P450 enzymes metabolizing oximes in the biosynthesis of glucosinolates in Arabidopsis.', *Plant physiology*, 133(1), pp. 63–72. doi: 10.1104/pp.102.019240.

Ogata, H., Goto, S., Sato, K., Fujibuchi, W., Bono, H. and Kanehisa, M. (1999) 'KEGG: Kyoto encyclopedia of genes and genomes', *Nucleic Acids Research*, pp. 29–34. doi: 10.1093/nar/27.1.29.

Ostell, J. and McEntyre, J. (2007) 'The NCBI Handbook', *NCBI Bookshelf*, pp. 1–8. doi: 10.4016/12837.01.

Pastore, J. J., Limpuangthip, A., Yamaguchi, N., Wu, M. F., Sang, Y., Han, S. K., Malaspina, L., Chavdaroff, N., Yamaguchi, A. and Wagner, D. (2011) 'LATE MERISTEM IDENTITY2 acts together with LEAFY to activate APETALA1', *Development*, 138(15), pp. 3189–3198. doi: 10.1242/dev.063073.

719 Pertea, M., Pertea, G. M., Antonescu, C. M., Chang, T.-C., Mendell, J. T. and Salzberg, S. L.
720 (2015) 'StringTie enables improved reconstruction of a transcriptome from RNA-seq reads',
721 *Nature Biotechnology*, 33(3), pp. 290–295. doi: 10.1038/nbt.3122.

722 Piñeiro, M., Gómez-Mena, C., Schaffer, R., Martínez-Zapater, J. M. and Coupland, G. (2003)
723 'EARLY BOLTING IN SHORT DAYS is related to chromatin remodeling factors and regulates
724 flowering in Arabidopsis by repressing FT.', *The Plant cell*, 15(7), pp. 1552–1562. doi:
725 10.1105/tpc.012153.

726 Ratcliffe, O. J., Kumimoto, R. W., Wong, B. J. and Riechmann, J. L. (2003) 'Analysis of the
727 Arabidopsis MADS AFFECTING FLOWERING gene family: MAF2 prevents vernalization by
728 short periods of cold.', *The Plant cell*, 15(5), pp. 1159–69. doi: 10.1105/tpc.009506.mous.

729 Robinson, M. D., McCarthy, D. J. and Smyth, G. K. (2010) 'edgeR: a Bioconductor package for
730 differential expression analysis of digital gene expression data.', *Bioinformatics (Oxford,*
731 *England)*, 26(1), pp. 139–40. doi: 10.1093/bioinformatics/btp616.

732 Saddic, L. A., Huvermann, B., Bezhani, S., Su, Y., Winter, C. M., Kwon, C. S., Collum, R. P. and
733 Wagner, D. (2006) 'The LEAFY target LMI1 is a meristem identity regulator and acts together
734 with LEAFY to regulate expression of CAULIFLOWER', *Development*, 133(9), pp. 1673–1682.
735 doi: 10.1242/dev.02331.

736 Sarid-Krebs, L., Panigrahi, K. C. S., Fornara, F., Takahashi, Y., Hayama, R., Jang, S., Tilmes,
737 V., Valverde, F. and Coupland, G. (2015) 'Phosphorylation of CONSTANS and its COP1-
738 dependent degradation during photoperiodic flowering of Arabidopsis', *Plant Journal*, 84(3), pp.
739 451–463. doi: 10.1111/tpj.13022.

740 Sayers, E. W., Barrett, T., Benson, D. A., Bryant, S. H., Canese, K., Chetvernin., V., Church, D.
741 M., Dicuccio, M., Edgar, R., Federhen, S., Feolo, M., Geer, L. Y., Helmberg, W., Kapustin, Y.,
742 Landsman, D., Lipman, D. J., Madden, T. L., Maglott, D. R., Miller, V., Mizrachi, I., Ostell, J.,
743 Pruitt, K. D., Schuler, G. D., Sequeira, E., Sherry, S. T., Shumway, M., Sirotkin, K., Souvorov,
744 A., Starchenko, G., Tatusova, T. A., Wagner, L., Yaschenko, E. and Ye, J. (2009) 'Database
745 resources of the National Center for Biotechnology Information', *Nucleic Acids Research*,
746 37(SUPPL. 1). doi: 10.1093/nar/gkn741.

747 Schwarz, S., Grande, A. V., Bujdoso, N., Saedler, H. and Huijser, P. (2008) 'The microRNA
748 regulated SBP-box genes SPL9 and SPL15 control shoot maturation in Arabidopsis', *Plant*
749 *Molecular Biology*, 67(1–2), pp. 183–195. doi: 10.1007/s11103-008-9310-z.

750 Shannon, P., Markiel, A., Ozier, O., Baliga, N. S., Wang, J. T., Ramage, D., Amin, N.,
751 Schwikowski, B. and Ideker, T. (2003) 'Cytoscape: A software Environment for integrated
752 models of biomolecular interaction networks', *Genome Research*, 13(11), pp. 2498–2504. doi:
753 10.1101/gr.1239303.

754 Siriwardana, N. S. and Lamb, R. S. (2012) 'The poetry of reproduction: The role of LEAFY in
755 Arabidopsis thaliana flower formation', *International Journal of Developmental Biology*, pp. 207–
756 221. doi: 10.1387/ijdb.113450ns.

757 Skylar, A., Matsuwaka, S. and Wu, X. (2013) 'ELONGATA3 is required for shoot meristem cell
758 cycle progression in Arabidopsis thaliana seedlings', *Developmental Biology*, 382(2), pp. 436–
759 445. doi: 10.1016/j.ydbio.2013.08.008.

760 Tarazona, S., García, F., Ferrer, A., Dopazo, J. and Conesa, A. (2012) 'NOIseq: a RNA-seq

761 differential expression method robust for sequencing depth biases', *EMBnet.journal*, 17(B), p.
762 18. doi: 10.14806/ej.17.B.265.

763 Trapnell, C., Roberts, A., Goff, L., Pertea, G., Kim, D., Kelley, D. R., Pimentel, H., Salzberg, S.
764 L., Rinn, J. L. and Pachter, L. (2012) 'Differential gene and transcript expression analysis of
765 RNA-seq experiments with TopHat and Cufflinks.', *Nature protocols*, 7(3), pp. 562–78. doi:
766 10.1038/nprot.2012.016.

767 Vitting-Seerup, K., Porse, B. T., Sandelin, A. and Waage, J. (2014) 'spliceR: an R package for
768 classification of alternative splicing and prediction of coding potential from RNA-seq data.', *BMC*
769 *bioinformatics*, 15, p. 81. doi: 10.1186/1471-2105-15-81.

770 Wang, B.-B. and Brendel, V. (2006) 'Genomewide comparative analysis of alternative splicing in
771 plants', *Pnas*, 103(18), p. 602039103. doi: 10.1073/pnas.0602039103.

772 Wang, L., Feng, Z., Wang, X., Wang, X. and Zhang, X. (2009) 'DEGseq: An R package for
773 identifying differentially expressed genes from RNA-seq data', *Bioinformatics*, 26(1), pp. 136–
774 138. doi: 10.1093/bioinformatics/btp612.

775 Yang, H. Q., Tang, R. H. and Cashmore, A. R. (2001) 'The signaling mechanism of Arabidopsis
776 CRY1 involves direct interaction with COP1.', *The Plant cell*, 13(12), pp. 2573–87. doi:
777 10.1105/tpc.010367.

778 Zhang, B., Wang, L., Zeng, L., Zhang, C. and Ma, H. (2015) 'Arabidopsis TOE proteins convey
779 a photoperiodic signal to antagonize CONSTANS and regulate flowering time', *Genes and*
780 *Development*, 29(9), pp. 975–987. doi: 10.1101/gad.251520.114.

781 Zhang, Z. H., Jhaveri, D. J., Marshall, V. M., Bauer, D. C., Edson, J., Narayanan, R. K.,
782 Robinson, G. J., Lundberg, A. E., Bartlett, P. F., Wray, N. R. and Zhao, Q. Y. (2014) 'A
783 comparative study of techniques for differential expression analysis on RNA-seq data', *PLoS*
784 *ONE*, 9(8). doi: 10.1371/journal.pone.0103207.

785 Zhao, S. and Zhang, B. (2015) 'A comprehensive evaluation of ensembl, RefSeq, and UCSC
786 annotations in the context of RNA-seq read mapping and gene quantification', *BMC Genomics*,
787 16(1), p. 97. doi: 10.1186/s12864-015-1308-8.

788

789

Figure and Tables

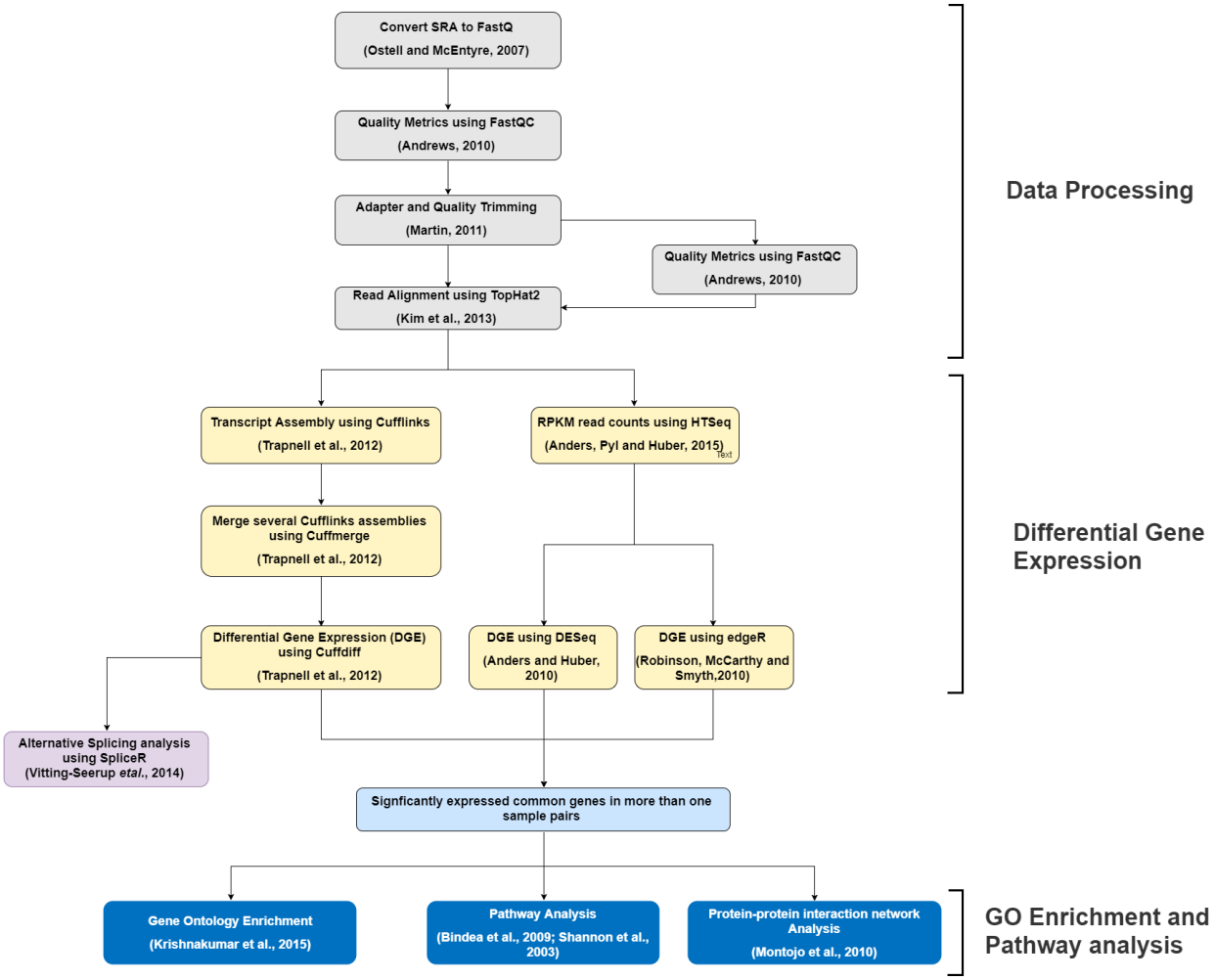

Fig. 1: Flowchart of the proposed RNA-Seq data analysis pipeline. The workflow is divided into three stages namely, data processing, differential gene expression and GO enrichment & network interaction analysis

a b

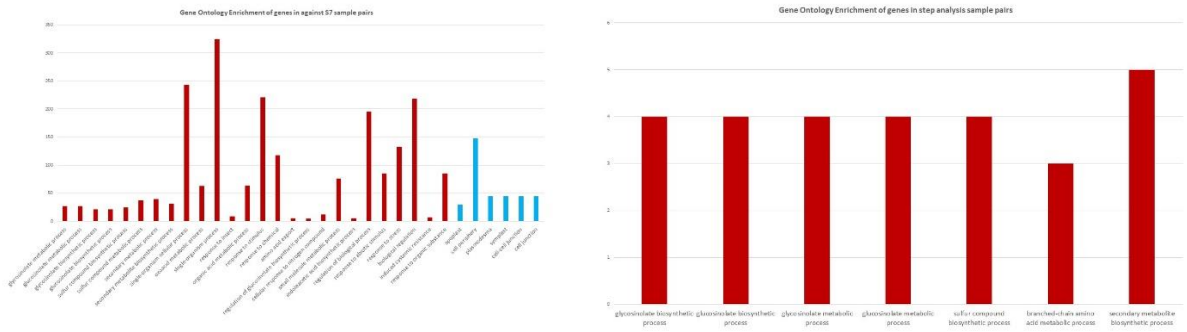

Fig. 2: GO enrichment functional classification results. The above figure illustrates classification of genes into several functional categories obtained using the Araport tool (Krishnakumar *et al.*, 2015). The genes obtained from Cuffdiff (Trapnell *et al.*, 2012), DESeq (Anders and Huber, 2010) and edgeR (Robinson, McCarthy and Smyth, 2010) are used for GO classification. (a) Illustrates GO classification results of common genes obtained from Cuffdiff, DESeq and edgeR for genes obtained from “Against S7” sample pairs. The bar chart contains two different gene ontologies. Bars colored in red represent genes enriched in “Molecular Function” whereas bars colored in blue represent genes enriched in “Cellular Component”, (b) GO classification results of common genes obtained from Cuffdiff, DESeq and edgeR for genes obtained from “Step Analysis” sample pairs. The bar chart only contains genes enriched in “Molecular Function” which are colored in red. Other two gene ontologies were not observed for the gene set provided from these sample pairs.

a

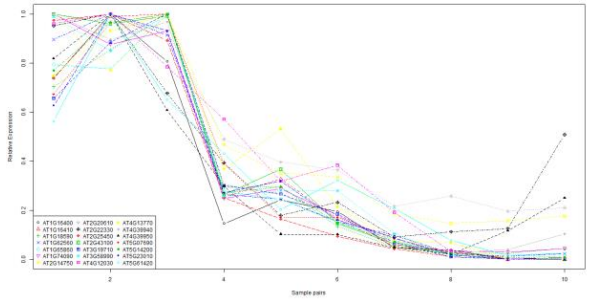

b

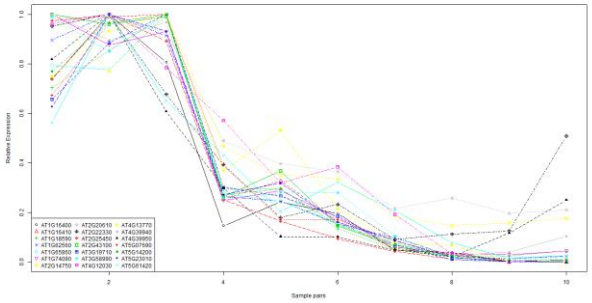

c

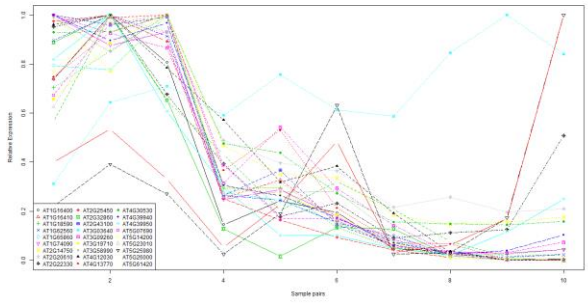

d

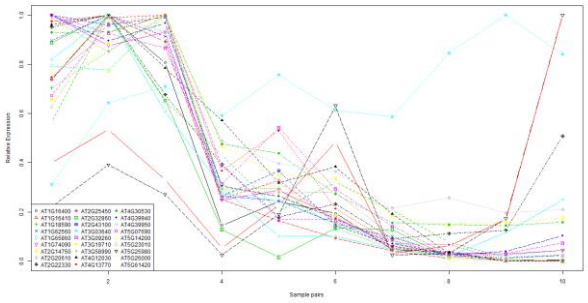

e

f

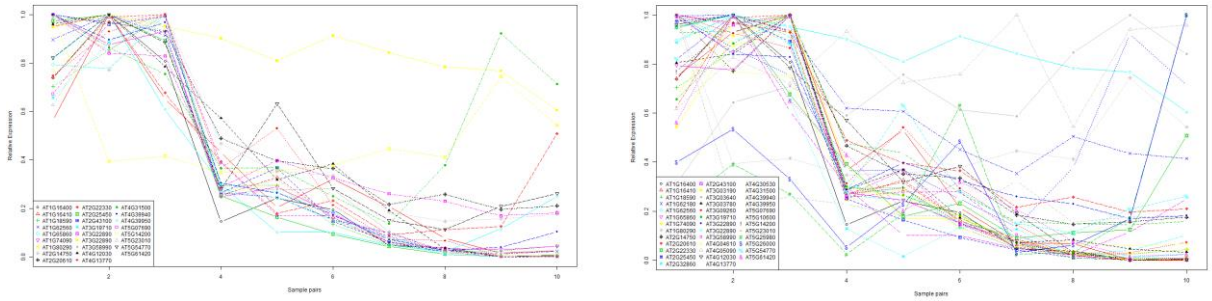

Fig. 3: Expression profiles of common genes from Cuffdiff-DESeq-edgeR overlap. The above graphs show expression profiles of genes enriched in glucosinolate biosynthetic process, glycosinolate biosynthetic process, glucosinolate metabolic process, glycosinolate metabolic process, sulfur compound biosynthetic process and sulfur compound metabolic process. (a) to (f) shows expression profiles of gene clusters in “Against S7” sample pairs. Common genes were obtained by overlapping DEGs from Cuffdiff (Trapnell *et al.*, 2012), DESeq (Anders and Huber, 2010) and edgeR (Robinson, McCarthy and Smyth, 2010) and expressed in more than one sample pairs.

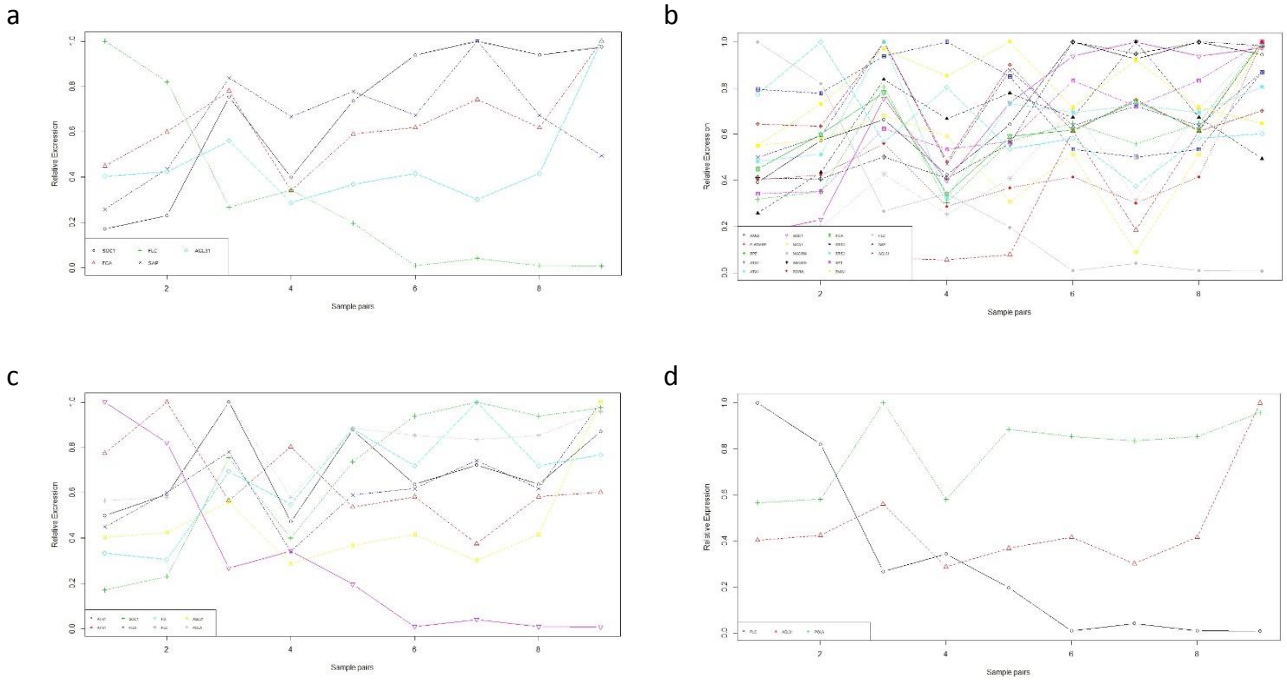

Fig. 4: Expression profiles of flowering genes. The above figure illustrates relative expression profiles of genes involved in flowering, flower development, regulation of flower development and negative regulation of flower development. (a), (b), (c) and (d) shows relative expression of genes in “Against S7” sample pairs

a b

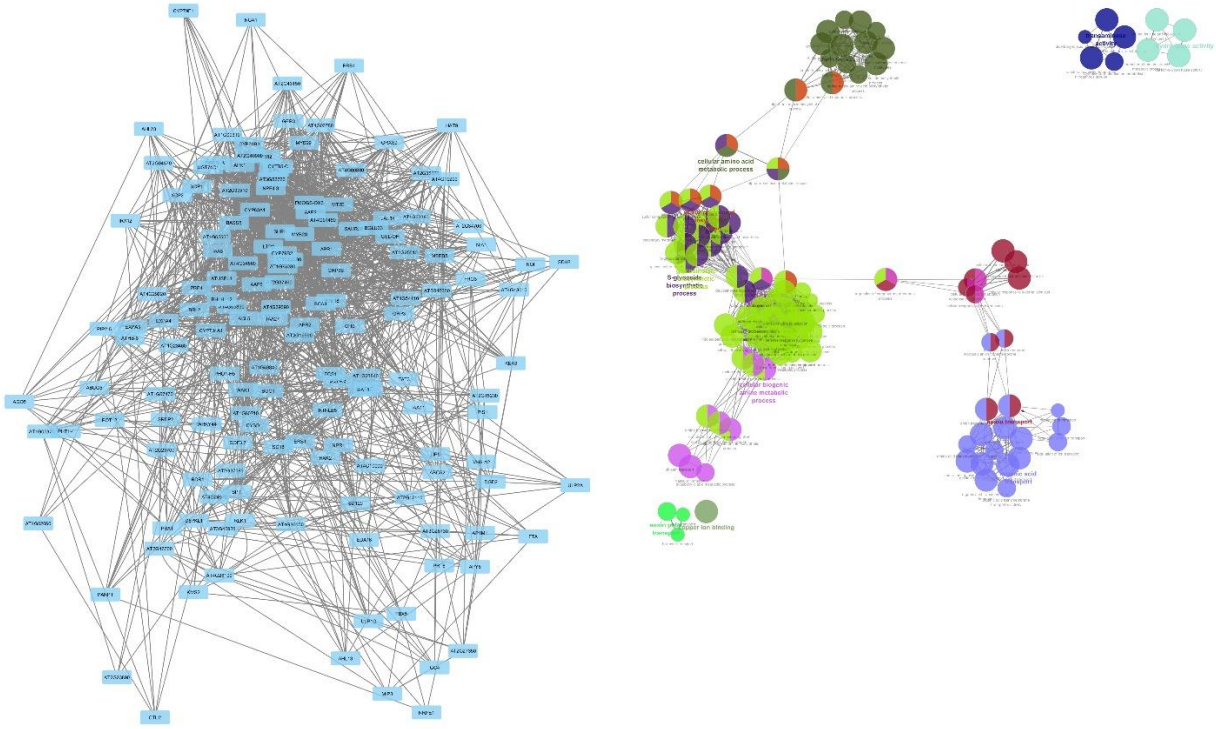

Figure 5: Protein-protein interaction network and Functional grouped network (FGN) of CGenes obtained from Cuffdiff-DESeq-edgeR overlap (Anders and Huber, 2010; Robinson, McCarthy and Smyth, 2010; Trapnell *et al.*, 2012). (a) PPI network obtained from GeneMania (Montojo *et al.*, 2010) showing interconnection and regulation of genes displayed by nodes which are colored in blue and edges colored in grey, (b) FGN obtained from ClueGO (Bindea *et al.*, 2009) with GOTerms as nodes linked based on kappa score where node size represents enrichment significance.

a

b

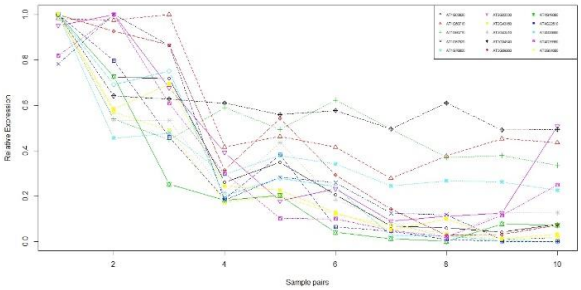

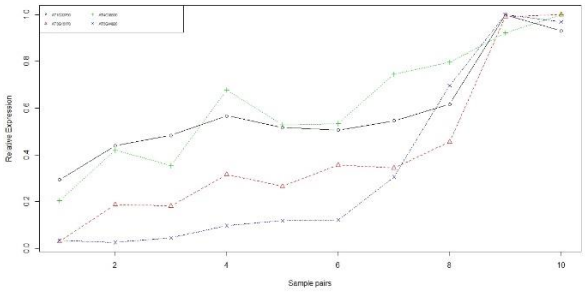

c

d

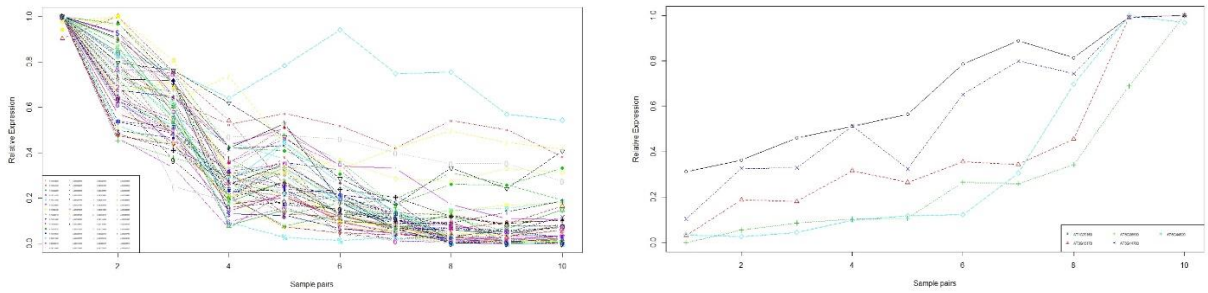

Fig. 6: Expression profiles of common genes from Cuffdiff-DESeq-edgeR (Anders and Huber, 2010; Robinson, McCarthy and Smyth, 2010; Trapnell *et al.*, 2012) overlap showing correlation to *FLC* and *LFY* genes. (a) shows DEGs showing higher correlation to *FLC* and regulation by *FLC*, (b) shows DEGs showing higher correlation to *LFY* and regulation by *LFY,* (c) shows DEGs having higher correlations to *FLC* and may or may not be regulated by *FLC*, (d) shows DEGs having higher correlations to *LFY* and may or may not be regulated by *LFY*

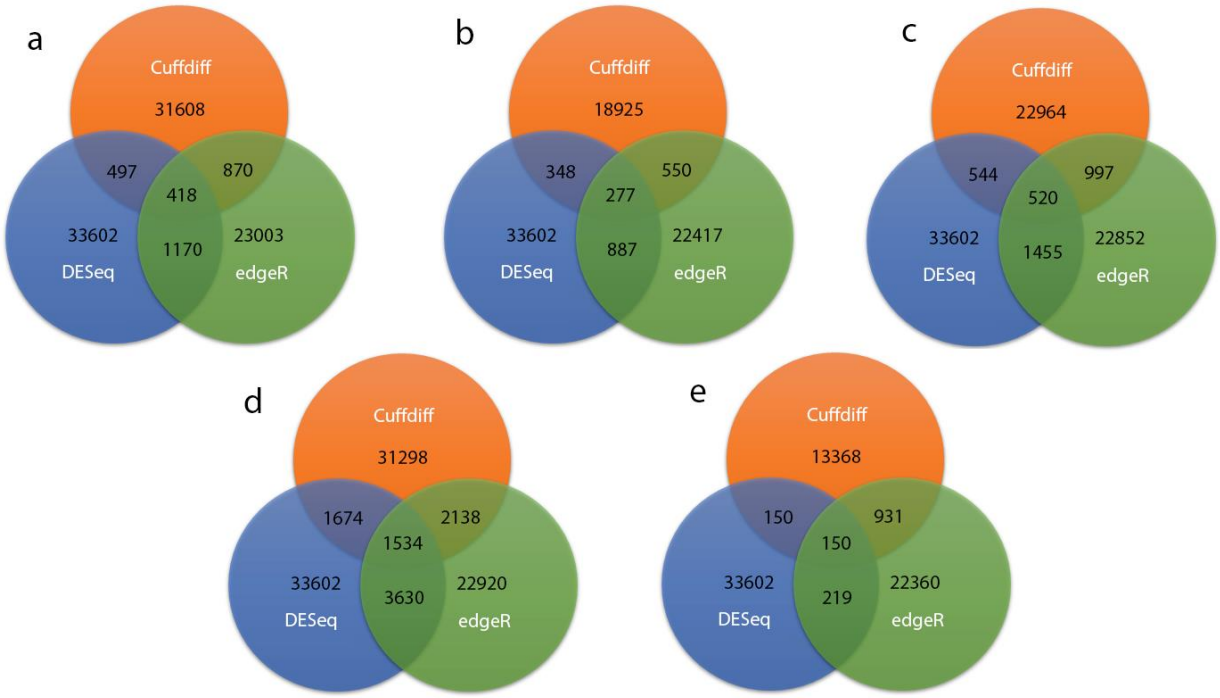

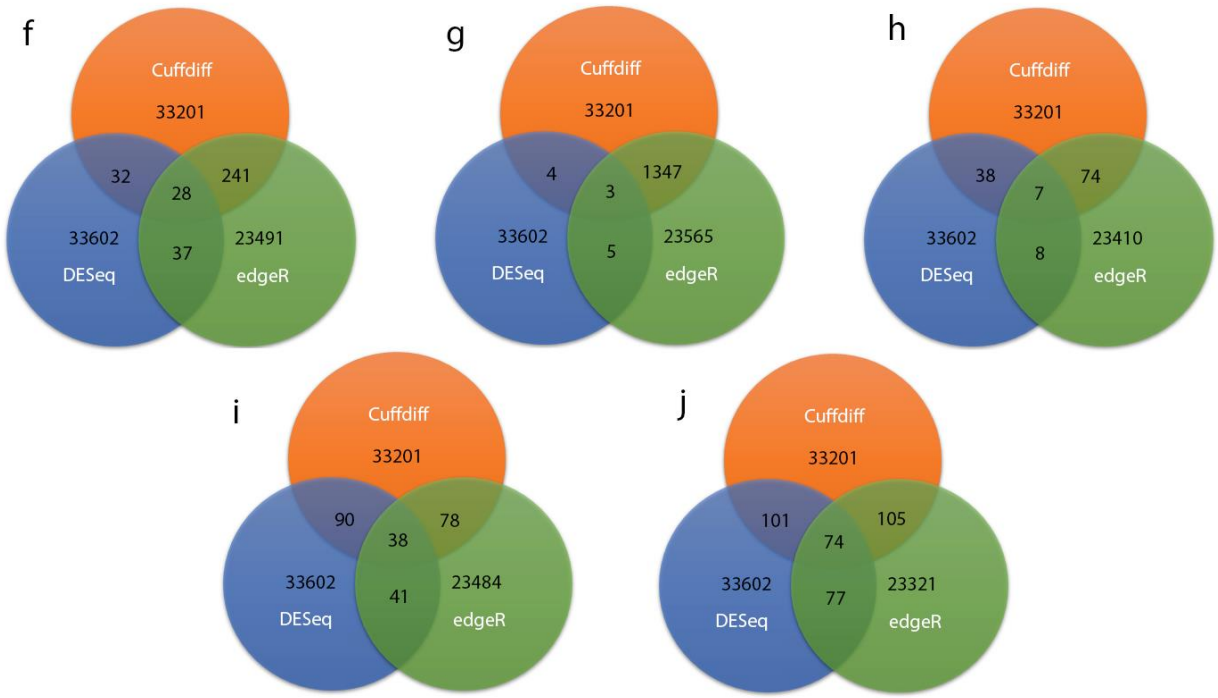

Fig. 7: Venn diagrams summarizing the overlap between Cuffdiff (Trapnell *et al.*, 2012), DESeq (Anders and Huber, 2010) and edgeR (Robinson, McCarthy and Smyth, 2010). (a), (b), (c), (d) and (e) shows overlapping genes from "Against S7" and (f), (g), (h), (i) and (j) shows overlapping genes from Step analysis. The overlapping genes are the DEGs in (a) S7-S10, (b) S7-S11, (c) S7-S12, (d) S7-S13, (e) S7-S14, (f) S9-S10, (g) S10-S11, (h) S11-S12, (i) S12-S13 and (j) S13-S14

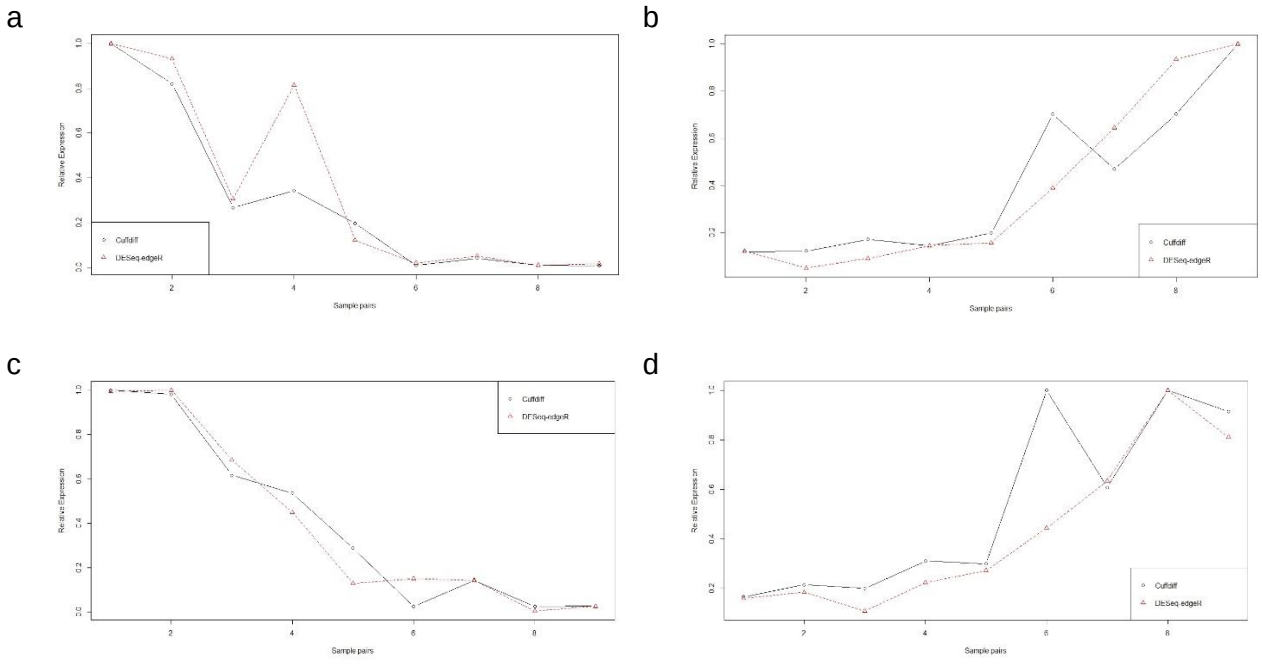

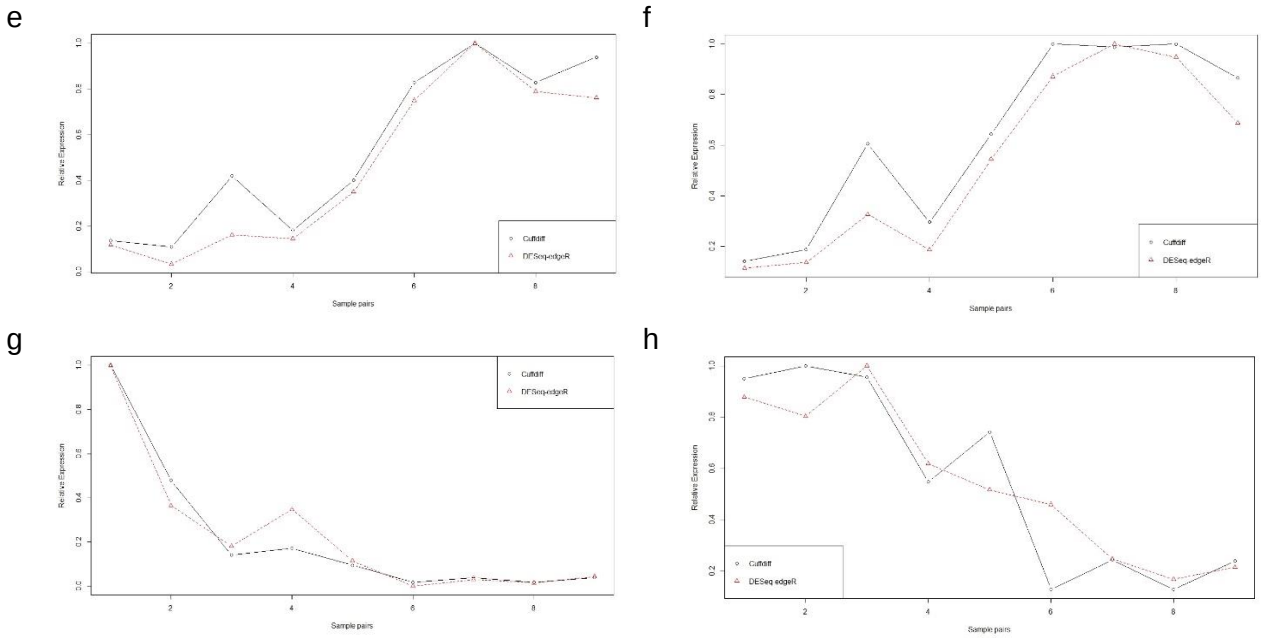

Fig. 8: Expression profiles of specific experimental genes in S7-S8, S7-S9, S7-S10, S7-S11, S7-S12, S7-S13, S7-S14, S7-S15 and S7-16 using Cuffdiff (Trapnell *et al.*, 2012) and DESeq (Anders and Huber, 2010) and edgeR (Robinson, McCarthy and Smyth, 2010) for (a) FLC, (b) LFY, (c) SMZ, (d) FPF1, (e) SPL9, (f) SPL15, (g) SNZ and (h) TOE2 genes

Table 1: List of some parameters used for reference alignment of reads using Tophat2. Each parameter contains their description, default value and the changed value for the analysis.

Flag	**Meaning**	**Default Value**	**Changed Value**
-i	The minimum intron length.	70 nt	40 nt
-I	The maximum intron length.	500000 nt	5000 nt
--segment-length	Each read is cut up into segments, each at least this long. These segments are mapped independently.	25 segments	20 segments
-g	Instructs TopHat to allow up to this many alignments to the reference for a given read, and choose the alignments based on their alignment scores if there are more than this number.	20 alignments	1 alignment
-a	The "anchor length".	8 bp	10 bp
-F	Minimum normalized depth	300 bp	0 bp

Table 2: Comparison chart for differential expression analysis. Two analyses were carried out: first, all samples were compared to day 7 (S7) when plants had two leaves visible; second, a step-wise analysis was done between two successive days.

Against S7	**Step analysis**
S7 vs S10	S9 vs S10
S7 vs S11	S10 vs S11
S7 vs S12	S11 vs S12
S7 vs S13	S12 vs S13
S7 vs S14	S13 vs S14

Table 3: Number of overlapping DEGs found in Cuffdiff, DESeq and edgeR results with FDR <= 0.05

Against S7					**Step analysis**				
Sample pairs	**Cuffdiff-DESeq-edgeR**	**Cuffdiff-DESeq**	**Cuffdiff-edgeR**	**edgeR-DESeq**	**Sample pairs**	**Cuffdiff-DESeq-edgeR**	**Cuffdiff-DESeq**	**Cuffdiff-edgeR**	**edgeR-DESeq**
S7-S10	418	497	870	1170	S9-S10	28	32	241	37
S7-S11	277	348	550	887	S10-S11	3	4	1347	5
S7-S12	520	544	997	1455	S11-S12	7	38	74	8
S7-S13	1534	1674	2138	3630	S12-S13	38	90	78	41
S7-S14	150	150	931	219	S13-S14	74	101	105	77

Table 4: List of filtered GO terms along with associated genes found in KEGG (Ogata *et al.*, 1999) and REACTOME (Croft *et al.*, 2014) databases obtained from ClueGO analysis (Bindea *et al.*, 2009) having Term PValue corrected with Benjamini-Hochberg < 0.05 for common genes obtained from “Against S7” sample pairs.

GOID	**GOTerm**	**Ontology Source**	**Term PValue Corrected with Benjamini-Hochberg**	**Group PValue Corrected with Benjamini-Hochberg**	**% Associated Genes**	**Nr. Genes**	**Associated Genes Found**
GO:0000261	Monobactam biosynthesis	KEGG	0.03	0.03	21.43	3.00	AK3, APS1, AT2G44040
GO:0000270	Cysteine and methionine metabolism	KEGG	0.01	0.00	10.10	10.00	ACO1, ACO2, AK3, ASP5, AT3G05430, CYSD1, HMT3, MS2, SERAT2;1, TAT3
GO:0000920	Sulfur metabolism	KEGG	0.00	0.00	19.51	8.00	AKN2, APK, APR1, APR2, APS1, AT4G05090, CYSD1, SERAT2;1
GO:0000290	Valine, leucine and	KEGG	0.02	0.02	17.39	4.00	BCAT4, IMD1, IPMI1, IPMI2

	isoleucine biosynthesis						
GO:0000660	C5-Branched dibasic acid metabolism	KEGG	0.02	0.02	30.00	3.00	IMD1, IPMI1, IPMI2
GO:0000380	Tryptophan metabolism	KEGG	0.02	0.00	13.04	6.00	CYP79B2, CYP79B3, CYP83B1, SUR1, TGG1, TGG2
GO:0000966	Glucosinolate biosynthesis	KEGG	0.00	0.00	57.89	11.00	BCAT4, CYP79B2, CYP79B3, CYP79F1, CYP79F2, CYP83A1, CYP83B1, MAM1, SOT17, SOT18, SUR1
GO:7438889	Cytosolic sulfonation of small molecules	REACTOME	0.02	0.16	16.00	4.00	AKN2, APK, SOT17, SOT18

Table 5: List of DEGs from Cuffdiff-DESeq-edgeR overlap (Anders and Huber, 2010; Robinson, McCarthy and Smyth, 2010; Trapnell *et al.*, 2012) showing higher correlations to *FLC* and *LFY* and status of regulation

Regulated by FLC and having higher correlation to FLC	**Not regulated by FLC but having higher correlation to FLC**	**Regulated by LFY and having higher correlation to LFY**	**Not regulated by LFY but having higher correlation to LFY**
AT1G03820, AT1G60710, AT1G67870, AT1G76800, AT2G22330, AT2G43150, AT2G43510, AT3G04940, AT3G09260, AT4G19380, AT4G22510, AT4G28660, AT4G39950, AT5G04080	AT1G04240, AT1G06090, AT1G14700, AT1G20850, AT1G28400, AT1G28710, AT1G51680, AT1G65500, AT1G67910, AT1G70940, AT2G01950, AT2G02010, AT2G14580, AT2G22800, AT2G23600, AT2G30080, AT2G37040, AT2G37170, AT2G37180, AT2G37460, AT2G37640, AT2G38080, AT2G38800, AT3G02910, AT3G05727, AT3G10120, AT3G21550, AT3G22740, AT3G25190, AT3G49780, AT3G53560, AT3G61210, AT3G62930, AT4G01390, AT4G04610, AT4G14465, AT4G22485, AT4G22513, AT4G22517, AT4G22520, AT4G22530, AT4G24060, AT4G31990, AT4G32880, AT4G34560, AT4G36570, AT5G43580, AT5G50200, AT5G51890, AT5G52050, AT5G59330, AT5G60780, AT5G63180, AT5G63710, AT5G64110	AT3G15170, AT5G44620, AT1G33790, AT4G36930	AT1G70160, AT5G06530, AT5G14700

873